ChemComm

COMMUNICATION

View Article Online
View Journal | View Issue

Cite this: *Chem. Commun.*, 2021, **57**, 8425

Received 7th June 2021,
Accepted 27th July 2021

DOI: 10.1039/d1cc02974f

rsc.li/chemcomm

Bioinspired *in situ* repeatable self-recovery of superhydrophobicity by self-reconstructing the hierarchical surface structure†

Md Ahsan Habib,[ab] Shuwang Wu,[ab] Qingrui Fan,[ab] Thomas Odey Magu,[ab] Xi Yao,*[c] Jianyong Lv*[ad] and Jianjun Wang*[ab]

Inspired by the biological self-recovery mechanism of superhydrophobicity, a new class of waxgel material with sustainable hierarchical surface micro-structures has been reported. After being damaged or removed, the waxgel material can self-reconstruct its surface layer both chemically and structurally, as well as successfully recovers its superhydrophobicity. In addition, it shows non-fluorinated composition, durability to severe mechanical challenges, and self-recoverable surface structures without external input of any kind such as; heat, UV, plasma *etc.*, which distinguishes waxgel from any previous self-healing superhydrophobic systems. This strategy will open a new path for improving the long-term functionality of different interfacial materials.

Superhydrophobic surfaces (SHSs) have attracted extensive interest during the past decades due to their unique water repellency and numerous promising potential applications.[1,2] To achieve superhydrophobicity, combining of low surface energy materials with delicate three-dimensional (3D) structure construction on the micro and/or nanoscale are necessary.[3] Low surface energy materials minimize water/solid interaction, and small-scale hierarchical surface micro/nano-structures are favorable to trap air at the solid/water interface raising the solid-to-water contact angle.[4] However, SHSs are often vulnerable to harsh environments (*e.g.*, sunlight exposure, oxidation, rain pour, sand abrasion, *etc.*),[2] and durability of the functionality is often challenging for the following reasons. First, the low-energy materials on the surfaces are susceptible to chemical deterioration; second, the delicately constructed structures can be easily damaged under external forces such as abrasion due to the small size and high aspect ratio. Furthermore, *in situ* self-recovery of the damaged low surface energy chemicals and *in situ* self-reconstruction of hierarchical surface structures, both are difficult or impossible by using the existing techniques until the materials are put in service;[5] such as plasma treatment,[6] heating,[7] *etc.* Besides, using fluorinated compounds for making water repellent materials is limiting due to the health hazardous issue.[8] Therefore, it is of great significance to develop new strategies and methodologies for designing and constructing fluorine-free durable SHSs.

Leaves and/or other parts of some land plants however can maintain their long-term functionalities such as superhydrophobicity *via* self-reconstructing the epicuticular wax layer. As shown in Fig. 1c, wheat leaf presents excellent superhydrophobicity with a water contact angle (CA) of 152°. This is because a rough and low surface energy epicuticular wax layer exists on the cuticular surface. Wheat leaf epicuticular wax is mainly a mixture of long-chain alcohols, alkanes, and fatty acids with different carbon numbers (C22 to C34); and assembles a layer with unique micrometer-sized crystal platelets.[9] After removing the wax platelets, CA decreases to 123° on the surface of the cuticle. But within 72 h, the leaf recovers its superhydrophobicity *via* reconstructing a new wax layer with the original morphology.

Inspired by the self-recovery nature of wheat leaf, herein we report a strategy to achieve repeatable *in situ* self-recovery of superhydrophobicity *via* designing a smart waxgel material that sustainably self-reconstructs its surface wax layer. After being damaged or removed, the wax layer is self-reconstructed both chemically and structurally without any external stimulus, as well as successfully recovers the superhydrophobicity. Notably, the self-reconstruction process smartly stops as long as the superhydrophobicity is achieved. To the best of our knowledge, this is the first time that a specific waxgel based bio-mimicking surface layer is self-reconstructed chemically and structurally to self-recover the surface functionality. This strategy will open a new path for improving the long-term functionality of biomimetic materials surface and interface.

[a] *Key Laboratory of Green Printing, Institute of Chemistry, Chinese Academy of Sciences, Beijing 100190, China. E-mail: wangj220@iccas.ac.cn, lvjianyong@iccas.ac.cn*
[b] *University of Chinese Academy of Sciences, Beijing 100049, China*
[c] *Key Laboratory for Special Functional Materials of Ministry of Education, School of Materials and Engineering, Henan University, Kaifeng 475000, China. E-mail: yaoxi@henu.edu.cn*
[d] *Songshan Lake Materials Laboratory, Dongguan 523808, Guangdong, China*

† Electronic supplementary information (ESI) available: Detailed preparation method of waxgel; characterization techniques; demonstration of self-cleaning feature of the waxgel material; identification of the wax composition by GCMS (PDF). See DOI: 10.1039/d1cc02974f

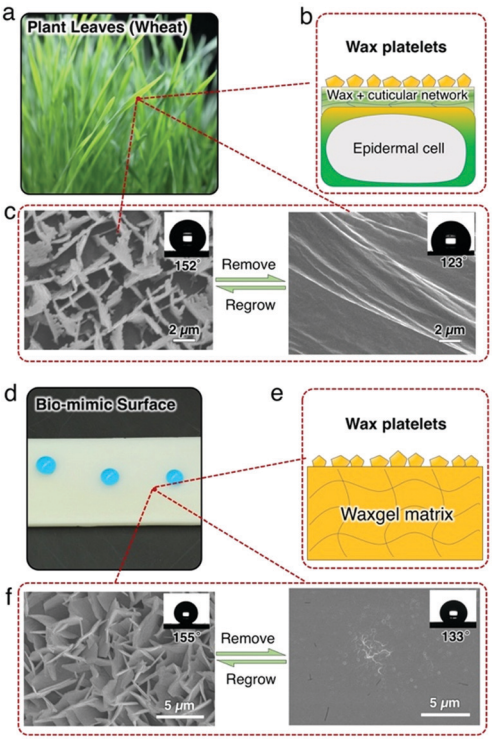

Fig. 1 Bio-inspired regrowth of wax structures. (a) The wheat leaf surface shows cuticular structures as indicated in (b). (c) The superhydrophobicity on wheat leaves is self-repaired because of the wax structure regrowth after physical challenge. (d) Inspired by plant cuticular structure recovery, we prepare an artificial cuticle based on waxgel. (e) The PDMS matrix exhibits a similar wax reservoir as the cuticle. (f) The wax structure on the waxgel surface exhibits self-growing behaviour after physical damage, similar to its natural counterpart (c).

Superhydrophobicity self-recovery of wheat leaves relies on the sustainable self-reconstruction of the epicuticular wax layer. As illustrated in Fig. 1b, wax is produced by epidermal cells and transported upward to the cuticle layer. The cuticle layers mainly comprise of a crosslinked 3D network of biomacromolecules (so-called ''cutin'') and serves as a reservoir of the wax. Then the wax assembles into crystalline platelets on the cuticle layer and gives rise to superhydrophobicity due to the low surface energy as well as the microscale hierarchical structure of the vertical platelets.[10,11] To mimic the functions of the wheat leaf system, a smart waxgel material that is capable of constructing a solid functional layer is designed and prepared in this work (Fig. 1d). To prepare such a waxgel, a piece of silicone rubber (polydimethylsiloxane, PDMS) is immersed in a bath of a wax mixture consisting of a typical fatty alcohol *n*-eicosanol-1 ($C_{20}H_{41}OH$, $C_{20}OH$ hereafter) and a typical long-chain alkane hexatriacontane (*n*-$C_{36}H_{74}$, hereafter C_{36}), and kept at ~150 °C for 6 hours (Fig. S2, ESI†). We choose 150 °C to ensure that both $C_{20}OH$ and C_{36} are liquids, and 6 hours is a minimum duration to reach swelling equilibrium at 150 °C (Fig. S2, ESI†). After reaching the swelling equilibrium, the swollen piece of silicone rubber is taken to the ambient environment at room temperature, with excess wax removed. As it cools down, we observe that the waxgel becomes opaque (white). Here the crosslinked PDMS matrix, in which the swollen wax is stored (Fig. 1e), resembles the epidermal cells and cutin of the wheat leaf system as shown in Fig. 1b. After a 12–24 hour period, the surface is uniformly covered by a snow-white wax layer and presents a similar appearance to the wheat leaf platelets (Fig. 1f). Removing such hierarchical structures reveals a smooth plane of wax. Interestingly, the wax platelets grow back in the ambient environment ~12–24 hours after removal, and the waxgel *in situ* self-recovers it's superhydrophobicity (Fig. 1f).

We attribute this structural regrowability to the continuous wax directional migration–crystallization cycle across the waxgel network, which closely resembles the natural design. And such a surface demonstrates easy self-cleaning feature (Fig. S3, ESI†), which is typical for a superhydrophobic surface.

To verify the self-recovering function, the wax structure is removed by adhesive tape. After removal, the superhydrophobicity is lost and the water contact angle (CA) reduces to ~133°, indicating that the wax platelet structure has been damaged. After standing still under ambient conditions for 24 hours, CA recovers to 154.6 ± 0.5°, which means the superhydrophobicity is fully recovered. We further repeat the damage-heal cycle on the same spot several times and find that the superhydrophobicity fully recovers up to 12 cycles (Fig. 2a), indicating the steady output of wax to the surface and repeatable construction of the platelet structure. Note that the maximum number of cycles for the self-regrowth is related to the amount of wax storage, which can be conveniently enhanced by opting for larger sample thickness, or higher swelling temperature.

The self-reconstruction process of the wax layer can be attributed to the sustainable wax directional migration/transportation from inside of the crosslinked matrix upward to the

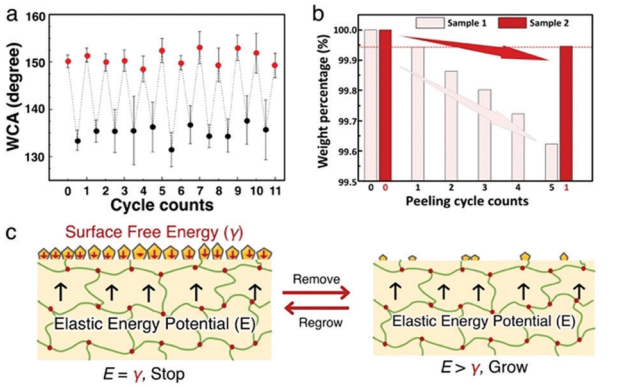

Fig. 2 The regrowth of the superhydrophobic structure on waxgel. (a) The regrowth process can be repeated for at least 12 cycles without losing superhydrophobicity. A steady weight loss is observed after each peeling operation for sample 1 with 24 hours-rest for the five cycles. Weight loss after 120 hours-rest (the sum of the total duration for five peeling operations for sample 1) for sample 2 is comparable to the weight loss of that of the first-cycle in sample 1 (b), indicating a smart regrowing strategy. (c) The smart regrowth is governed by energy balance. Wax migration is driven by excessive elastic energy potential *E*, which stops when *E* is balanced to the surface energy γ, exerted by wax platelet formation.

surface, which closely resembles the natural leaf system. To understand the mechanism better, weight loss of waxgel in cyclic peeling operation is compared with a duration interval of 24 hours between two adjacent cycles. Two almost identical samples (samples 1 and 2) are taken and weight losses are measured followed by adhesive tape peeling operation. It is found that there is almost a steady weight loss from one cycle to the next, which implies a consistent production of wax platelets (sample 1 in Fig. 2b). Platelets from sample 2 are, however, peeled only once after sample 1 reaches its five peeling operation cycles. Interestingly, in the case of 120 hours time duration by the end of the first cycle (as in sample 2), the amount of weight loss is comparable to that after the first 24 hours duration in sample 1. This result indicates that rather than keep growing uncontrollably, the platelet growth could stop at the point of achieving surface superhydrophobicity, and the next growing cycle will only be reactivated upon new physical damage. Therefore, the waxgel material exhibits a capability of smartly self-regulating the superhydrophobicity self-recovery upon repeated physical damage on the surfaces. And this self-regulating damage-dependent construction of the wax layer is of significant importance for sustainable self-recovery of superhydrophobicity.

We explain this smart regrowing feature by analyzing the energy transfer processes during waxgel preparation as well as wax platelet formation. As shown in Fig. 2c, the elastic potential E exerted by the swelling PDMS network is balanced by the total surface free energy γ of wax platelets atop, which scales with the total area of wax platelets. After platelet removal, the surface free energy reduces significantly due to the loss of rough surfaces. As a result, the elastic potential becomes unbalanced, which drives wax diffusion from inside to the surface of the waxgel.[12] As new platelets continue to form, γ increases accordingly until a new balance is reached, which eventually stops the wax migration process. Such a curious case of smart self-repair strategy driven by thermal dynamics might also be helpful in deciphering the physical mechanism of plant wax structural regulation on natural surfaces.[13]

To understand how the $C_{20}OH$-to-C_{36} wax ratio governs the surface wax morphology, we quantify the wax composition at several key spots (inside/on-top and in the bath) by gas chromatography-mass spectroscopy (GCMS) (Fig. S4–S8, ESI†). As indicated in the central graph in Fig. 3, the wax composition inside the gel is similar to that in the bath, indicating that the diffusivity of C_{36} and $C_{20}OH$ molecules in the PDMS network is similar at 150 °C. However, the wax composition on top (24 h release time) evolves differently from the one in the bath. Specifically, the concentration of C_{36} on the surface does not increase significantly until its concentration in the bath (and inside the gel) increases to above 90%. This concentration mismatch between C_{36} and $C_{20}OH$ is due to the higher polarity of $C_{20}OH$ than that of C_{36}, which alters the migration rate in the PDMS network significantly at room temperature, *i.e.* $C_{20}OH$ tends to migrate out faster from the non-polar PDMS network.[14,15] Therefore, we need to increase the C_{36}-to-C_{20}OH ratio (>90%) during preparation, to achieve a comparable

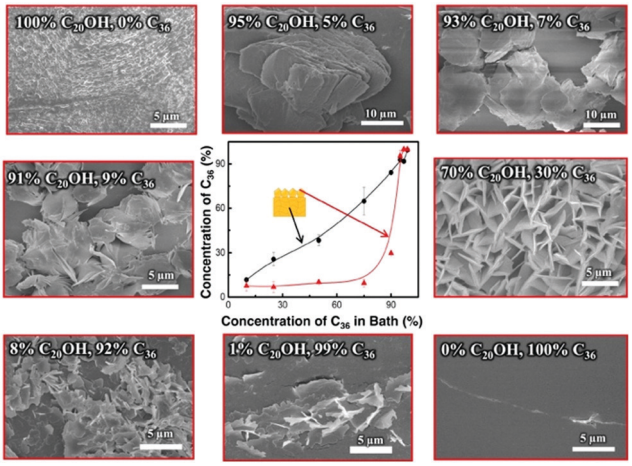

Fig. 3 Influence of wax composition on the waxgel surface morphology. Graphs showing C_{36} concentration inside (black curve) and on top (red curve) of the waxgel as changing the one in the bath. Due to diffusion rate difference at room temperature, the ratio of C_{36} on the surface is always lower than that in the waxgel inside. And the C_{36} on top does not increase significantly until that in the bath is sufficiently high (>90%). SEM images showing that the wax platelet structure does not appear until the C_{36} concentration (~30%) becomes comparable to that of $C_{20}OH$, and disappears in the case of pure C_{36}, which indicates that a significant proportion of C_{36} on the waxgel surface is a prerequisite for the formation of a wax platelet structure. All SEM images are taken here ~24 h after the waxgel preparation.

C_{36}-to-$C_{20}OH$ ratio at the waxgel surface. This mismatch provides a guideline for effectively producing the wax platelet structure, as we later find that there is a lower limit on the C_{36} concentration in the wax, below which the platelets do not form. Also, as shown in Fig. 3, we find that the surface exhibits different morphologies as changing the wax composition on top of the waxgel. Specifically, when the content of C_{36} is <30%, there are large wax granules with irregular shapes on the surface are noticed. However, when C_{36} reaches 30%, well-defined wax platelets appear. After that, although a higher amount of C_{36} is present on the waxgel surfaces but, due to the presence of less amount of $C_{20}OH$ the platelets density decreases. Above all, to achieve a wax platelet structure, the C_{36}, and $C_{20}OH$ content should be comparable on top, which requires a high concentration (≥90%) of C_{36} in the bath.

To understand the platelet growth mechanism on a molecular level, we observe the platelet re-generation process by SEM. (Fig. 4). First, we categorize the different stages of wax structure formation. At 0.2 h, the waxgel surface is covered by an in-plane wax layer. This in-plane wax layer is also found after platelet removal (Fig. 1f). At 1 h, scales of wax platelets emerge, indicating that the out-of-plane wax crystal formation has started. At 6 h, the surface is fully covered by wax platelets with larger size compared to those observed at 1 h. Based on the above observation, we divide the surface wax growing process into three stages. As shown in Fig. 4b–d: (I) in-plane layer formation, when the wax molecules diffuse to the waxgel surface and form a thin wax layer, (II) platelet initiation, when vertical growth starts, and (III) the platelets maturing, when the

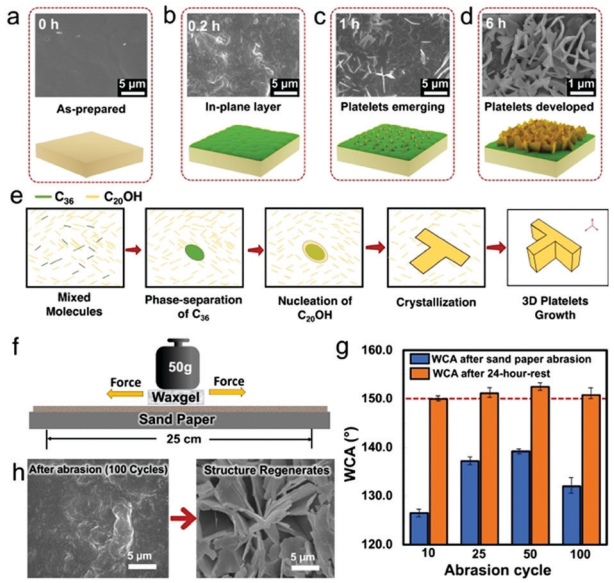

Fig. 4 The process of wax platelet formation on waxgel. (a) The as-prepared waxgel surface is smooth. (b) At 20 min a layer of wax is observed. (c) At 60 min platelets start to emerge from the surface. (d) At 360 mins, platelets fully form and cover the surface. (e) Insight into platelet formation at the microscopic level. Firstly, the solvent-like C_{36} + $C_{20}OH$ mixture migrates to the surface. Secondly, C_{36} phase-separates from the mixtures and forms crystal seeds. Thirdly, $C_{20}OH$ molecules nucleate around the C_{36} seeds and form crystal platelets. (f) The waxgel slides against sandpaper cyclically. (h) After 100 cycles of abrasion followed by a 24 hours-rest, the platelets grow back. (g) The self-recovery of superhydrophobicity is evident for various cycle numbers of the sandpaper abrasion.

platelets are fully grown and completely cover the waxgel surface. To find the reason for this structure, we consider the crystallization behavior in our case in analogy to the case when wax crystallizes from its melt, assuming that the wax in the matrix transfers to the surface in a quasi-liquid state.[16] In our system, the amount of $C_{20}OH$ molecules is associated with a smaller carbon number, but a larger amount and higher polarity compared to C_{36} molecules. Therefore, during crystallization, C_{36} molecules phase-separate from the quasi-liquid, crystallized first which act as seeds. This leads to heterogeneous crystallization.[17] $C_{20}OH$ then starts nucleating around the C_{36} seeds, which further leads to crystallization and 3D crystal platelet formation.[18]

Due to the 3D-homogeneous composition, the waxgel should be able to produce wax platelet structures on any exposed surface. In other words, superhydrophobicity is regrowable, even if the pre-existing surface has been completely depleted by some severe physical challenges.

To verify, we rub the waxgel against the surface of sandpaper (600 mesh) under a normal load of 50 g for several cycles. The results show that the superhydrophobicity was lost right after the abrasion, but fully restored after resting for 24 h in all cases, which is due to the regrowth of platelet structures (Fig. 4g).

Superhydrophobicity is a unique property that we've learnt from nature for decades. Now our next task is clear: figuring out an efficient mechanism to realize structural self-repair. In this work, we take this challenge by mimicking the natural design and strategy, which is to regrow wax platelet structures based on an artificial cuticle material, *i.e.* the waxgel. Advantages include fully recoverable structure and superhydrophobicity over many cycles (depending on the storage capacity or size of the material), smart damage-triggered regrowth, high sustainability (due to the eco-friendly nature of wax), and low cost. We investigate the wax crystal platelet formation mechanism, which mainly involves impurity-manipulated anisotropic crystallization. Understanding the crystallization pattern gives the opportunity to further develop this system with diverse materials (waxes, polymers, surfactants, salts, *etc.*) and functions that can be extended from the self-cleaning area to others like micro/nano machining, template-based bio-assay, *etc.* Acknowledging such an autonomous, damage-triggered self-recovering system creates a unique opportunity in gaining deeper insights into the crop survival strategies and possible routes to improve them. Furthermore, the success in the current exploration set up a standard protocol in designing smart self-regulating systems, from which we can draw several key principles: (1) continuous raw material supply (wax in our case), (2) structure formation based on a spontaneous process (such as recrystallization), and (3) a stopping mechanism to cease each growing cycle. Above all, we consider this work as a start for a broadening subject in the long run.

The authors are grateful for the financial support from the National Natural Science Foundation of China (21805286 and 21905077) and the National Defense Science and Technology Special Zone Innovation Project (17-163-12-ZT-003-085-01). In addition, Md Ahsan Habib would also like to acknowledge the financial contribution for his study and research work supported by CAS-TWAS Presidents' Fellowship (NO. 2016CTF027).

Conflicts of interest

The authors have no conflicts of interest.

References

1 X. Zhang and F. Shi, *et al.*, *J. Mater. Chem.*, 2008, **18**, 621–633.
2 K. Manoharan and S. Bhattacharya, *Journal of Micromanufacturing*, 2019, **2**(1), 59–78.
3 L. Feng and S. Li, *et al.*, *Adv. Mater.*, 2002, **14**, 1857–1860.
4 S. Parvate and P. Dixit, *et al.*, *J. Phys. Chem. B*, 2020, **124**, 1323–1360.
5 M. Ghasemlou and F. Daver, *et al.*, *J. Mater. Chem. A*, 2019, **7**, 16643–16670.
6 Y. Li and L. Li, *et al.*, *Angew. Chem., Int. Ed.*, 2010, **122**, 6265–6269.
7 X.-J. Guo and C.-H. Xue, *et al.*, *J. Mater. Chem. A*, 2019, **7**, 17604–17612.
8 Í. G. M. d. Silva and E. F. Lucas, *et al.*, *Macromol. Mater. Eng.*, 2020, **305**, 202000400.
9 K. Koch and W. Barthlott, *et al.*, *Planta*, 2006, **223**, 258–270.
10 A. Stosch and A. Solga, *et al.*, *J. Appl. Bot. Food Qual.*, 2007, **81**, 49–55.
11 L. Kunst and R. Jetter*et al.*, *Annual plant reviews, biology of the plant cuticle*, 2006, pp. 182–207.
12 S. Nah and A. Thomas, *Rubber Chem. Technol.*, 1981, **54**, 255–265.
13 C. Neinhuis and K. Koch, *et al.*, *Planta*, 2001, **213**, 427–434.
14 T. M. Aminabhavi and R. S. Munnolli, *et al.*, *Polym. Int.*, 1995, **36**, 353–363.
15 S. S. Choi, *J. Appl. Polym. Sci.*, 1999, **73**, 2587–2593.
16 A. Volynskii and T. Y. Grokhovskaya, *et al.*, *Polym. Sci.*, 1988, **30**, 2220–2227.
17 S. Karthika and T. Radhakrishnan, *et al.*, *Cryst. Growth Des.*, 2016, **16**, 6663–6681.
18 J.-L. Li and R.-Y. Wang, *et al.*, *J. Phys. Chem. B*, 2009, **113**, 5011–5015.

